Iranian Journal of Medical Physics
Vol. 10, No. 3, Summer 2013, 118-132
Received: April 25, 2013; Accepted: Aug 14, 2013

Original Article

Autonomous Drug-Encapsulated Nanoparticles: Towards a Novel Non-Invasive Approach to Prevent Atherosclerosis

Alireza Rowhanimanesh[1*], Mohammad Reza Akbarzadeh Totonchi[1]

Abstract

Introduction
This paper proposes the concept of autonomous drug-encapsulated nanoparticle (ADENP) as a novel non-invasive approach to prevent atherosclerosis. ADENP consists of three simple units of sensor, controller (computing), and actuator. The hardware complexity of ADENP is much lower than most of the nanorobots, while the performance is maintained by the synergism in the swarm architecture.
Materials and Methods
Since high accumulation of low density lipoprotein (LDL) macromolecules within the arterial wall plays a critical role in the initiation and development of atherosclerotic plaques, the task of the swarm of ADENPs is autonomous feedback control of LDL level in the interior of the arterial wall. In this study, we consider two specific types of ADENPs with distinguishing capabilities. The performance of each type is evaluated and compared on a well-known mathematical model of the arterial wall through computer simulation.
Results
Simulation results demonstrate that the proposed approach can successfully reduce the LDL level to a desired value in the arterial wall of a patient with very high LDL level that is corresponding to the highest rates of cardiovascular disease events. Moreover, it is shown that ADENP is capable of distinguishing between healthy and unhealthy arterial walls to reduce the drug side effects.
Conclusion
The proposed approach is a promising autonomous non-invasive method to prevent and treat complex diseases such as atherosclerosis.

Keywords: Atherosclerosis, Low Density Lipoprotein, Nonlinear Control, Swarm Control, Nanoparticles.

1- *Department of Electrical Engineering, Center of Excellence on Soft Computing and Intelligent Information Processing (SCIIP), Ferdowsi University of Mashhad, Mashhad, Iran.*
*Corresponding author: Tel: +98 (511) 8806027; email: rowhanimanesh@ieee.org

1. Introduction

Global drug delivery as a non-invasive method, angioplasty as a minimally-invasive approach, and open surgery as an invasive medical procedure are the most common techniques for prevention and treatment of atherosclerosis (or hardening of the arteries) that is one of the major causes of death in humans. In some patients, these conventional methods cannot permanently prevent and treat the disease and some new atherosclerotic plaques may be developed in other places of the coronary arteries. Recent advances in nanomedicine leads to manufacturing of drug-encapsulated nanoparticles (DENPs) that can selectively deliver drugs to a specific organ or tissue. Local drug delivery by DENPs reduces unwanted side effects and thus increases the variety in choosing the type and dosage of drug. In recent years, DENPs have received significant attention as a promising non-invasive approach to prevent and treat atherosclerosis in contrast to the conventional methods [1].

Hamzeh et al. demonstrated that their designed targeted drug-encapsulated nanoparticles (DENPs), 80 nm in length and 30 nm in width, could successfully enter the interior of the atherosclerotic plaques to deliver the drugs and imaging agents in laboratory mice [2]. Lu et al. have experimentally shown on laboratory mice that mesoporous silica nanoparticles, with spherical shape and $100-130$ nm in diameter, have rapid excretion from animal body through urine and feces, suggesting a quick and complete clearance of nanoparticles by the animal body [3]. The pioneering works of Freitas on nanorobotics proposed a desirable medical nanorobot structure for targeted drug delivery [4]. Suraj and Reddy proposed an algorithm for navigation of the nanorobots towards the blood clot in the constricted arteries [5]. Hossain et al. mathematically modeled the transport of coupled drug molecules and DENPs in coronary artery walls [6, 7]. Martel employed magnetic nanoparticles and a specific MRI platform to design a swarm of synthetic microscale nanorobots that are capable of traveling in the blood circulatory network [8]. Nakano et al. formulated the dynamics of local drug delivery by a nanoparticle-eluting stent and compared its efficiency with the conventional stents [9]. Nakano et al. theoretically considered the dynamic motion of the magnetic nanoparticles in blood vessels and demonstrated that it could be controlled by external magnetic fields [10]. Dutta et al. exploited the heat that is generated by iron-oxide nanoparticles in presence of external magnetic field to melt the atherosclerotic plaque [11]. Furthermore, Cavalcanti and his colleagues used chemical and thermal gradients to navigate nanorobots towards the coronary occlusion [12].

Generally, these previous works are classified into two categories: DENPs and nanorobots [13-15]. Although DENPs can be manufactured today, they have limited capabilities and cannot deal with complex tasks. In contrast, the capabilities of a nanorobot are much higher than a DENP, but most of the suggested architectures for nanorobots are too complex and not realizable by today's nanotechnology. As a trade-off between performance and hardware complexity, this paper proposes ADENP that can be more reasonably realized technologically. The hardware complexity of ADENP is lower than most of the nanorobots, while the performance is maintained by the synergism in the swarm architecture. The swarm of ADENPs can be directly injected into the blood stream, naturally transported by blood flow, and entered into the interior of the arterial wall through natural diffusion/advection like biological macromolecules. Since high accumulation of low density lipoprotein (LDL) macromolecules within the arterial wall plays a critical role in the initiation and development of atherosclerotic plaques, the task of the swarm of ADENPs is autonomous feedback control of the LDL level in the interior of the arterial wall [16]. It should be noted that the goal of the proposed approach is to quickly reduce the LDL level in the interior of the arterial wall, not in the blood (lumen), to

prevent critical growth of atherosclerotic plaque. Thus, this method is mainly designed for the patients with very high LDL level ($> 200\, mg\ \mathrm{dL}^{-1}$) who are corresponding to the highest rates of cardiovascular disease events [17]. In contrast to the existing targeted DENPs that usually target the surface proteins of atherosclerotic plaques, the ADENPs directly sense the concentration signals such as LDL and drug levels in the interior of the arterial wall, and hence it can diagnose abnormal LDL accumulation before plaque formation. It is important to note that in this paper, we consider a nanoparticle as a system and our insight to ADENP is abstract and mathematical. Indeed, ADENP introduces a general abstract model for a class of DENPs, not a specific DENP with certain materials and physical-chemical structure. Therefore, different types of ADENPs can be designed as shown in the next section. Moreover, the proposed approach is general and can be used for the treatment of different diseases such as cancer and stroke, not only limited to atherosclerosis.

2. Materials and Methods

The anatomical structure of arterial wall is schematically illustrated in Figure 1. The important layers that play critical role in atherosclerosis are endothelium, intima, internal elastic lamina (IEL), and media. In this study, the drug is defined as a chemical compound which tends to combine with LDL, and the products of this reaction could be excreted from the body through renal excretion. Our insight to drug is abstract and mathematical and we do not consider a certain drug with specific chemical/physical properties. ADENP and drug molecule are assumed to be spherical particles of 100 nm and 4 nm in diameter, respectively. The previous experimental studies in [2] and [3] confirm that the assumed size for ADENP in this study is applicable.

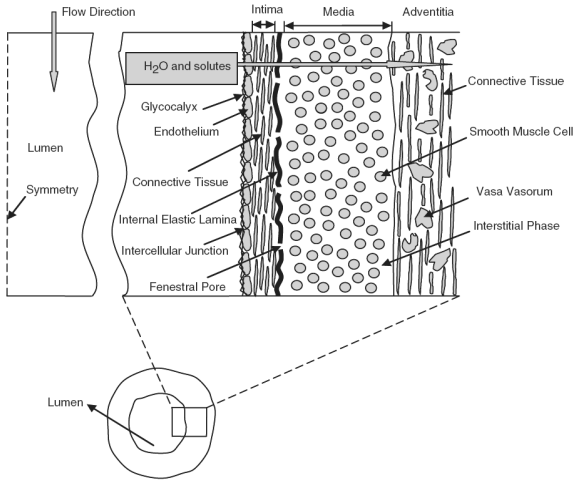

Figure 1. Transverse section of the arterial wall [16].

2.1. LDL-ADENP-Drug Transport in Arterial Wall

There exist different mathematical models in the literature for macromolecule transport in the arterial wall. The present study utilizes the four-layer model introduced by Yang and Vafai due to its generality and robustness [16]. Their model has been also used in other researches such as in [1, 6, 7, 18, and 19]. Inspired by that model, authors in [1] have introduced a general mathematical model for LDL-DENP-Drug transport in the arterial wall. According to the proposed model by authors in [1], the governing equations of LDL, ADENP, and drug transport within the arterial wall are [1].

$$\frac{\partial C^{l}_{LDL}}{\partial t} = -\left(1-\sigma^{l}_{fLDL}\right)V_{filt}\nabla C^{l}_{LDL} + D^{l}_{LDL}\nabla^{2}C^{l}_{LDL} - k^{l}_{rLDL}C^{l}_{LDL} - R_{y}(C^{l}_{LDL}, C^{l}_{drug}) \quad (1)$$

$$\frac{\partial C^{l}_{drug}}{\partial t} = -\left(1-\sigma^{l}_{fdrug}\right)V_{filt}\nabla C^{l}_{drug} + D^{l}_{drug}\nabla^{2}C^{l}_{drug} - k^{l}_{rdrug}C^{l}_{drug} - R_{z}\left(C^{l}_{LDL}, C^{l}_{drug}\right) + m\, C^{l}_{ADENP}\, u \quad (2)$$

$$\frac{\partial C^{l}_{ADENP}}{\partial t} = -\left(1-\sigma^{l}_{fADENP}\right)V_{filt}\nabla C^{l}_{ADENP} + D^{l}_{ADENP}\nabla^{2}C^{l}_{ADENP} - k^{l}_{rADENP}\, C^{l}_{ADENP} \quad (3)$$

where l is the layer number (from endothelium ($l = 1$) to media ($l = 4$)), ∇ the gradient, ∇^2 the laplacian, V_{filt} the filtration velocity, and the reaction between LDL and drug is modeled by R_y and R_z. C^{l}_{LDL}, σ^{l}_{fLDL}, D^{l}_{LDL}, and k^{l}_{rLDL} are the concentration, filtration reflection coefficient, effective diffusivity, and reaction coefficient, respectively, for LDL in the l^{th}

layer. The similar notation is used for drug and ADENP. m is the mass of a drug molecule, k_{rdrug} and k_{rADENP} the reaction coefficients of drug, and ADENP with the environment. u is the drug release rate (molecule s^{-1}) by each ADENP and manipulated with the controller unit of ADENP.

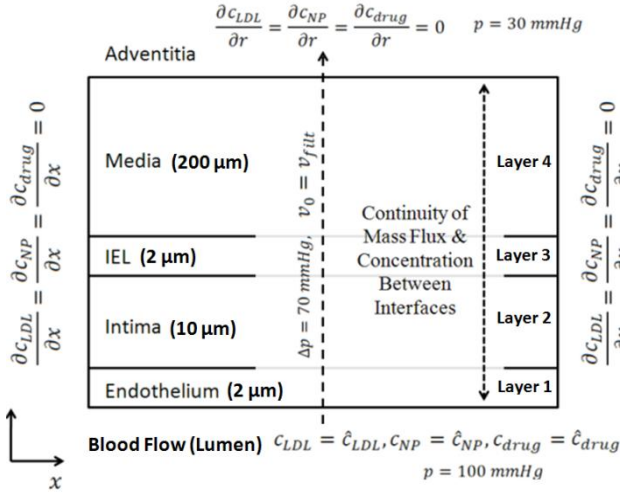

Figure 2. The boundary conditions used in the numerical simulation.

According to [16], advection and diffusion play the main role in transport of macromolecules/particles from blood to arterial wall as well as within the inside of the arterial wall. Moreover, reaction is an important phenomenon which considerably takes effect on the concentration of macromolecules/particles in the interior of the arterial wall. Equations 1-3 mathematically model all of these three phenomena for LDL, drug, and ADENP, respectively. For example, in Equation 1, advection, diffusion, and reaction of LDL macromolecules are modeled by $-(1-\sigma^{l}_{fLDL})V_{filt}\nabla C^{l}_{LDL}$, $D^{l}_{LDL}\nabla^2 C^{l}_{LDL}$, and $-k^{l}_{rLDL}C^{l}_{LDL}$, respectively. Moreover, the term $-R_y(C^{l}_{LDL}, C^{l}_{drug})$ models the reaction between LDL and drug. Similar terms are used in Equations 2 and 3 for drug and ADENP. In Equation 2, the term $m\,C^{l}_{ADENP}\,u$ models the drug release by ADENPs. Figure 2 represents the boundary conditions at the interfaces between wall layers, where the continuity of mass flux and concentration is considered. The details of model description and physiological parameters are presented in [1].

2.2. Autonomous DENP

Autonomous DENP (ADENP) consists of three simple units of sensor, controller, and actuator (Figure 3). This structure enables ADENP to continuously sense the human body and autonomously release the required drug if any abnormality occurs. Due to this autonomy, the proposed DENP is called 'Autonomous DENP' in comparison with conventional DENPs. In this paper, we consider a nanoparticle as a system and our insight to ADENP is abstract and mathematical. Indeed, ADENP introduces a general abstract model for a class of DENPs, not a specific DENP with certain materials and physical-chemical structure. Therefore, different types of ADENPs can be designed.

Two of the most common approaches for non-invasive prevention and treatment of atherosclerosis are global drug delivery and targeted DENPs. We consider the capabilities of these two methods from the viewpoint of control theory. Global drug delivery is open-loop control. Since in this method, the drug is directly released in the blood flow, only small dosages of drug are usually administered to prevent drug toxicity. Using global drug delivery, a trivial mass of drug is transported to the interior of the arterial wall, while approximately the whole of the drug mass is consumed in the lumen. Since no autonomous feedback is taken from LDL accumulation and available drug within the arterial wall, this method cannot distinguish between unhealthy (abnormal) and healthy (normal) arterial walls and the drug is released blindly (open loop control). This drawback could dangerously increase the unwanted side effects on healthy tissues as well as inefficient drug consumption. Although treatment by global drug delivery is economically much cheaper than treatment by DENPs, the above-mentioned drawbacks reduce the effectiveness of this method. In contrast to global drug delivery, targeted DENP is semi-closed-loop control. In this procedure, targeted DENPs exploit protein bindings (or similar cases) to target specific tissue for local drug delivery.

These targeted bindings play the role of feedback from the unhealthy tissue. Most of the existing targeted DENPs target the surface molecules of an inflamed plaque and this can sometimes be a big limitation for this method. In many cases, the plaque inflammation is trivial or in the early stages, but there is a very high accumulation of LDL in the interior of the arterial wall. In these cases, due to the low density of the desired proteins (required for binding) on the plaque surface, the performance of targeted DENPs is not good. In general, since feedback is not taken from LDL and drug, this method is open loop with respect to LDL and drug. As a result, some of the drawbacks of global drug delivery are still available for this method, but with less degree. In comparison with these two common approaches, a swarm of ADENPs can autonomously take feedback from both LDL and drug concentrations in the interior of the arterial wall and realize closed-loop control at nanoscale. This ability of autonomous feedback control makes ADENP an effective approach for early prevention of atherosclerotic plaque formation and development.

Figure 3 depicts the structure of ADENP. The hardware complexity of these units should be low for more reasonable manufacturing within the existing bounds of technologies. In contrast to a nanorobot, ADENP does not contain any propulsion unit, while it exploits natural diffusion/advection for locomotion such as macromolecules. It should be noted that ADENP is designed based on the concept of swarm control for collective problem solving in swarm manner. This means that ADENP is not designed to work individually, while it is proposed for swarm control. In comparison with a nanorobot, ADENP individually has very limited capabilities particularly from computing aspects (weak controller unit). But a swarm of ADENPs exploits swarm control which gives it some emerging capabilities to be as strong as a group of multiple nanorobots. It is noteworthy that the hardware complexity of ADENP is usually much lower than a nanorobot. The sensor unit of ADENP includes one or more nanoscale molecular concentration sensors to sense concentration signals such as C_{LDL}, and C_{drug} from the environment (e.g. interior of the arterial wall). The actuator unit of ADENP contains a controllable drug pump (or a controllable drug valve) that is connected to drug payload to release the drug molecules in the aqueous environment with a flow rate determined by the controller unit. The most important part of ADENP is controller unit. Controller unit determines which concentration signals are sensed by ADENP, and how drug release rate (output of ADENP) is changed according to the sensed values. Indeed, controller unit is the decision making unit of ADENP and should be a simple mapping to be realizable in the nanoscale. The effect of controller unit is mathematically modeled as the control signal u in Equation 2. Depending on the controller unit, different ADENPs can be proposed such as PDENP and SPDENP that are considered later. Generally, a swarm of ADENPs can include few groups of ADENPs which differ in computing, sense, and actuation units.

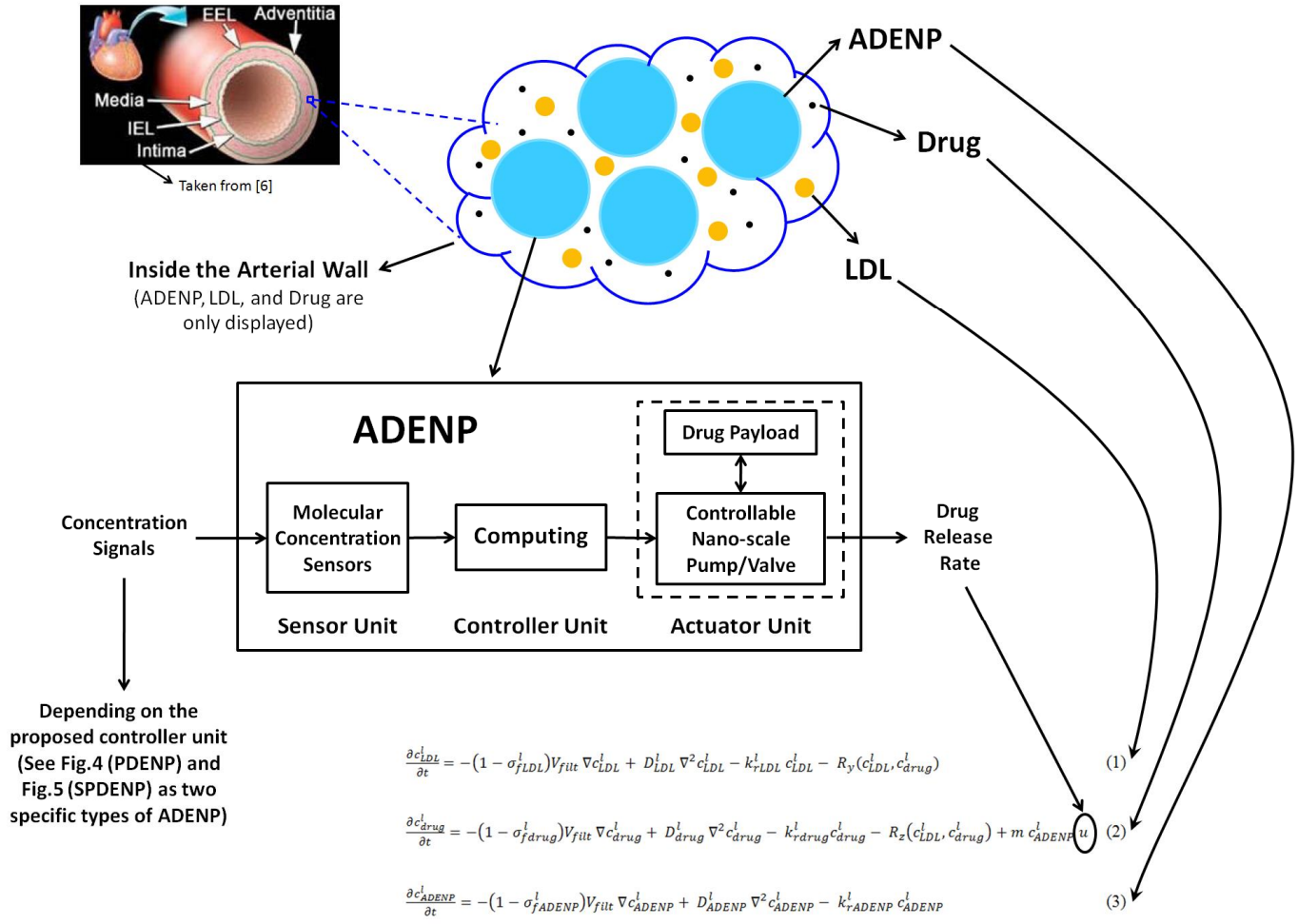

Figure 3. The general structure of ADENP

It is assumed that ADENP has a limited lifetime (above few days). Biodegradability is considered as the clearance mechanism of ADENP. After the lifetime of ADENP is finished (even if ADENP is still full of drug), ADENP is broken into small biocompatible molecules (similar to the waste products of metabolism) which can be cleared from living tissues through natural clearance mechanism of human body. This ensures that ADENPs are always cleared from human body especially from deep tissues like Media and lymph nodes. Also, ADENP can have an additional subsystem of artificial lysosome that is conceptually similar to a natural lysosome. When the ADENP is empty of drug (released the whole of its encapsulated drug), the artificial lysosome releases its encapsulated enzymes inside the ADENP, and consequently the ADENP is rapidly broken and dissolved in the aqueous environment. It is important to note that although our insight to ADENP is abstract and mathematical, the materials that are used in ADENP must guarantee biocompatibility especially after biodegradation.

2.2.1. Experimental Feasibility

There exist many research works in the literature such as the pioneering works of Freitas and Cavalcanti in medical nanorobotics that have just proposed theoretical basis and hypothetical structure for their nanorobots [12-15]. Some of those theoretical designs cannot be implemented by today's nanotechnology yet. However, ADENP carries simpler hardware architecture in order to be more reasonably realized technologically. In recent years, many remarkable experimental works have been performed on construction of

computing unit, sensors, and actuators at nanoscale. Since ADENP consists of molecular concentration sensors, a nanoscale computing unit and a nanometer-sized controllable valve, we just briefly reviewed several of those state-of-the-art experimental works which have been done on the construction of these specific nanoscale devices during the past three years.

Beginning from the most recent, in 2013, Li et al. used DNA strand displacement to design majority logic gate and multiple input logic circuits as a promising approach for synthesis of nanometer-sized computational units [20]. In DNA nanotechnology, the component materials are strands of nucleic acids such as DNA, which are well-suited to nanoscale construction because a nucleic acid double helix has a diameter of 2 nm and a helical repeat length of 3.5 nm with about 10-12 base pairs per turn, where the length of a base pair is approximately 0.34 nm [43]. Yasuga et al. described microfluidic logic gates which use DNA and biological nanopores and they could successfully realize NAND gates [21]. In nanotechnology, a nanopore is ranged from about one to few nanometers in diameter [42]. Chan et al. employed MRI-detectable pH nanosensors incorporated into hydrogels for in vivo sensing of transplanted-cell viability [22]. Iscla et al. improved the design of an MscL (large-conductance mechanosensitive channels)-based triggered nanovalve which can be widely used as an actuator for nanoscale applications [23]. MscL as pore-forming membrane proteins can translate the physical forces to electrophysiological signals. The pore diameter of MscL in the open state has been estimated to be about 3 nm, which accommodates the passage of small proteins. Lai et al. designed specific mesoporous silica nanoparticles for real-time monitoring of drug release [24]. Mesoporous silica nanoparticles are manufactured today as applied nanoscale devices with controlled particle size in a very wide range from 20 nm to 700 nm [44].

In 2012, Douglas et al. described an autonomous logic-gated DNA nanorobot for targeted transport of molecular payloads to cells [25]. Miyamoto et al. proposed a new approach for synthesis of Boolean logic gates in living mammalian cells [26]. Their designed gates can produce output signals such as fluorescence and membrane ruffling on a timescale of seconds, substantially faster than earlier intracellular logic gates. Bonnet et al. proposed an approach for rewritable digital data storage in live cells via engineered control of recombination directionality in DNA [27]. Padirac et al. constructed a two-input switchable memory element and a single-input memory circuit based on DNA biochemistry [28]. Their results suggest that it is possible to build complex time-responsive molecular circuits. Jonoska et al. reviewed two computing models by DNA self-assembly whose proof of principal had recently been experimentally confirmed [29]. The first model is a finite-state automaton with output where gold nanoparticles (ranging from about ten to few hundreds of nanometers) are assembled to read-out the result. In the second model, a complex DNA molecule representing a graph emerges as a solution of a computational problem. Lakin et al. presented a programming language for designing DNA strand displacement devices [30]. Strand displacement techniques enable computational devices (from logic gates, to chemical reaction networks, to architectures for universal computation) to be implemented in DNA without the need for additional components, allowing computation to be programmed solely in terms of nucleotide sequences [30].

Agrawal et al. reviewed recent advances in nanosensors and their pharmaceutical application [31]. Lorenzo et al. proposed a specific nanosensor for sensing ultralow concentrations of the targeted molecule [32]. They demonstrated the outstanding sensitivity and robustness of their approach by detecting an ultralow concentration of the cancer biomarker prostate-specific antigen. Khanna considered the physical, chemical, and biological aspects of nanosensors as well as the recent advances in this technology [33]. Du et al. designed a biocompatible drug delivery nanovalve system on the surface of

mesoporous nanoparticles [34]. Long et al. considered recent research progress on the construction of supra-molecular nanovalves, installed on the surface of mesoporous nanomaterials, which could effectively control the targeted release of encapsulated cargo molecules, such as drug molecules, anti-cancer drugs, and oligonucleic, under external stimuli [35]. Xue et al. demonstrated that lysozyme molecules can act as a pH-responsive nanovalve for the controlled release of guest molecules from mesoporous silica [36].

In 2011, Tasmir et al. combined a simple genetic circuit with quorum sensing to produce more complex computations in space [37]. They constructed a simple NOR logic gate in E. coli. Individual colonies of E. coli carry the same NOR gate, but the inputs and outputs are wired to different orthogonal quorum-sensing 'sender' and 'receiver' devices. The quorum molecules form the wires between gates. By arranging the colonies in different spatial configurations, all possible two-input Boolean logic gates are produced. E. coli is a rod-shaped bacterium whose length and diameter are about 2 μm and 0.5 μm, respectively. Qian et al. applied DNA strand displacement for designing digital logic circuits at nanoscale [38, 39]. They experimentally demonstrated several digital logic circuits, culminating in a four-bit square-root circuit that comprises 130 DNA strands. Al-Fandi et al. proposed a living biological nanorobot as a self-navigator sensor for diseases [40]. Yang et al. worked on the properties of MscL nanovalves which can be considered as a widely-used triggered nanovalve for targeted drug release devices [41].

Generally, although the size of components in some of these works is not less than 100 nm (the nominal size of ADENP), they are promising enough to demonstrate that smaller nanoscale components will be manufactured in near future to be applicable in ADENP. As a result, recent advances in nanotechnology ensure that manufacturing of ADENP will be experimentally feasible.

2.2.2. Two Specific Types of ADENPs

Authors have already proposed two advanced DENPs that can be considered as two specific types of ADENPs with distinguishing characteristics including Proportional DENP (PDENP) and Sliding-Based Proportional DENP (SPDENP) [1, 45]. SPDENP is designed analytically based on mathematical proof, and its robust performance is mathematically proven in the presence of uncertainty. However, PDENP is designed through simulation without any mathematical proof. Generally, SPDENP is more robust than PDENP. PDENP senses both LDL and drug concentrations and exploits a piece-wise linear controller to reduce LDL level in the arterial wall, while SPDENP senses LDL concentration and its derivative, and exploits nonlinear sliding-based proportional controller. SPDENP does not have sensor for drug concentration, hence leading to simpler design. In contrast, since PDENP takes feedback from drug, it can reduce the unwanted drug side effects in healthy tissue. Moreover, due to the dynamics of its controller unit, PDENP is stronger than SPDENP in distinguishing between healthy and unhealthy tissues. In the following sections, we consider each of these ADENPs, briefly.

2.2.2.1. Proportional DENP (PDENP)

Figure 4 depicts the structure of PDENP. The sensor unit senses LDL concentration (C_{LDL}) and drug concentration (C_{drug}) from the environment. The controller unit is a simple memoryless piecewise-linear mapping. Drug pump releases the drug molecules in the aqueous environment with a flow rate determined by the controller unit. When a PDENP finishes its drug payload, it should be removed and replaced by new PDENPs. For this reason, we consider an artificial lysosome inside the PDENP that is conceptually similar to a natural lysosome. When the PDENP is empty of drug, the artificial lysosome releases its encapsulated enzymes inside the PDENP, and consequently the PDENP is rapidly broken and solved in the aqueous environment. The dynamics of the controller unit of PDENP is as follows:

$$u = \begin{cases} \text{poslin}\left(k_{L1}(C_{LDL} - 100) - k_d C_{drug}\right) & 100 \le C_{LDL} \le 160 \\ \text{poslin}\left(k_{L2} C_{LDL} - k_d C_{drug}\right) & 0 \le C_{LDL} \le 10 \\ 0 & \text{otherwise} \end{cases} \quad (4)$$

Where C_{LDL} and C_{drug} are the values of the LDL and drug concentrations in the environment and are measured by the sensors of the PDENP, u is the drug release rate, and:

$$\text{poslin}(x) = \begin{cases} x & x > 0 \\ 0 & x \le 0 \end{cases} \quad (5)$$

k_{L1}, k_{L2}, and k_d are the adjustable parameters of this controller that are designed according to the desired performance such as drug delivery rate. PDENP is designed for patients with vey high LDL level ($> 200\ mg\ dL^{-1}$). To prevent releasing drug in lumen, u is set to zero for $C_{LDL} > 160\ mg\ dL^{-1}$. Thus, PDENPs do not release any drug in lumen and the lower positions of Endothelium in which C_{LDL} is above $160\ mg\ dL^{-1}$. Also, to prevent releasing drug in healthy arterial walls, u is set to zero for $C_{LDL} < 100\ mg\ dL^{-1}$, where the peak of the normal LDL concentration is $\sim 100\ mg\ dL^{-1}$. To exploit the PDENPs that are transported to Intima, IEL and Media, u is nonzero but small for $C_{LDL} \le 10\ mg\ dL^{-1}$, corresponding to the LDL level in these layers. Also, to increase the efficiency of drug release, a feedback is taken from C_{drug}, and u is linearly decreased by increasing C_{drug}.

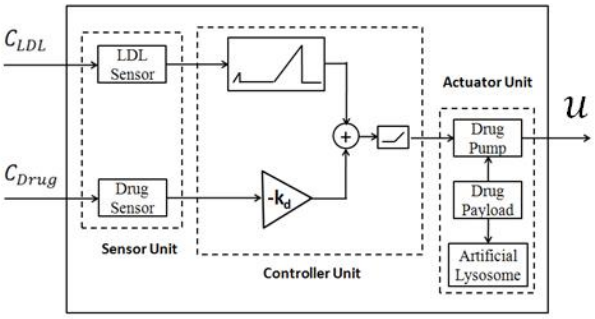

Figure 4. The structure of PDENP as a specific type of ADENP.

2.2.2.2. Sliding–based Proportional DENP (SPDENP)

Sliding-mode control theory is a powerful analytical approach to prove the stability and performance of swarms [46-49]. Figure 5 shows the structure of SPDENP. The sensor unit senses C_{LDL} and $\frac{dC_{LDL}}{dt}$ from the environment. The controller unit of SPDENP is basically a biased proportional controller, while some nonlinear term is added to increase the smoothness of the controller. This controller unit is analytically designed based on a new nonlinear lumped mathematical model for mass transport in the arterial wall that has been proposed by authors and the concepts of sliding-mode control theory. The stability and robustness of this controller has been mathematically proven. In SPDENP, it is assumed that the capacity of the drug payload of SPDENP is large enough such that it does not empty during the lifetime of SPDENP. Simulation results demonstrate that the drug consumption of SPDENP is lower than PDENP. The dynamics of the controller unit of SPDENP is as follows:

$$u = \begin{cases} \left(1 - \frac{C_{LDL}}{160}\right) u_c & s > s_c \quad \text{and} \quad C_{LDL} < 160\ mg\ dL^{-1} \\ \left(1 - \frac{C_{LDL}}{160}\right)\left(\frac{s}{s_c}\right) u_c & 0 \le s \le s_c \quad \text{and} \quad C_{LDL} < 160\ mg\ dL^{-1} \\ 0 & \text{otherwise} \end{cases} \quad (6)$$

where $s = \frac{dC_{LDL}}{dt} + \lambda\, C_{LDL}$ (the sliding surface), where C_{LDL} and $\frac{dC_{LDL}}{dt}$ are the values of the LDL concetration and its derivative in the environment and are measured by the sensors of the SPDENP, and u is the drug release rate. $\lambda > 0$, $s_c > 0$, and $u_c > 0$ are the adjustable parameters of this controller that are designed according to the desired performance. It should be noted that large values of u_c enhance the robustness of controller in the presence of uncertainty. Moreover, large values of u_c and λ increase the controller speed. However, if the values of these design parameters are set to large values, it considerably increases the drug consumption that is challengeable in practice. Thus, a trade-off should be considered between robustness, speed, and drug consumption. Similar to PDENP, SPDENP is designed for patients with very high LDL level ($> 200\ mg\ dL^{-1}$) and hence the term $160\ mg\ dL^{-1}$ is appeared in the controller equation.

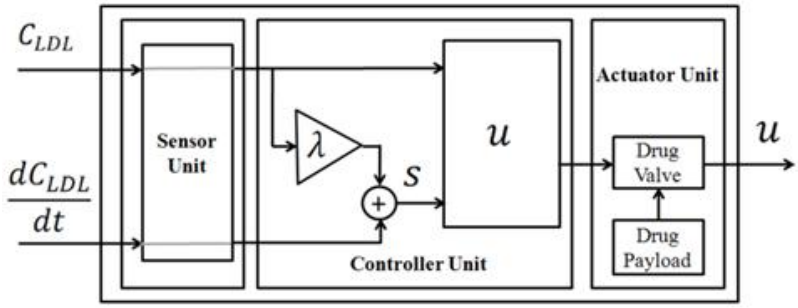

Figure 5. The structure of SPDENP as a specific type of ADENP.

2.3. Simulation

In order to demonstrate the capabilities of ADENPs in swarm control of living systems, in this paper, a swarm of ADENPs is employed to control the LDL level in the arterial wall of a patient with very high LDL level through computer simulation. The mathematical model of the previous section has been simulated numerically with the mesh size of 100 nm and time step of 10 s in MATLAB (version 2008). The details of the numerical technique which we have used for solving Equations 1-3 can be found in [50]. It is presumed that the proposed ADENPs are administrated to a patient with very high LDL level. Thus, the LDL concentration in lumen, $\hat{c}_{LDL}$, is assumed to be $200\ \mathrm{mg\,dL^{-1}}$ that is medically known as 'very high LDL level' [17]. We take the concentration of ADENP and drug in blood (lumen) as $\hat{c}_{ADENP} = 200\ \mu\mathrm{g\,mL^{-1}}$ and zero, respectively. Lu et al. reported that at concentrations below $100\ \mu\mathrm{g\,mL^{-1}}$, mesoporous silica nanoparticles do not induce any cytotoxicity in a variety of cell lines, and some growth inhibition was noted when the concentration exceeds $200\ \mu\mathrm{g\,mL^{-1}}$ [3]. Thus, the value of $\hat{c}_{ADENP}$ in the present study is applicable. The initial values of ADENP and drug concentrations in the interior of the arterial wall are set to be zero. In this simulation, $k_{rdrug} = 10^{-4}\mathrm{s^{-1}}$, $k_{rADENP} = 10^{-6}\mathrm{s^{-1}}$, $m = 4.98 \times 10^{-20}\mathrm{g}$ that is $\sim$100 times smaller than the mass of an LDL molecule, $R_y(C_{LDL}, C_{drug}) = k_{rLDLdrug} C_{LDL} C_{drug}$, $R_z(C_{LDL}, C_{drug}) = k_{rdrugLDL} C_{LDL} C_{drug}$, and $k_{rdrugLDL} = 0.01\, k_{rLDLdrug} = 10^{3}\mathrm{mm^3 g^{-1} s^{-1}}$. The mass of each ADENP is assumed to be 60000 times larger than m. It is presumed that the fluid velocity V is just nonzero towards r axis (Fig. 2), and equals to the filtration velocity, that is, $V_{filt} = 1.67 \times 10^{-5}\mathrm{mm\,s^{-1}}$ for the transmural pressure of 70 mmHg [7, 16]. Without loss of generality, in the present simulation, a one-dimensional model is used in which signals are spatially dependent to r axis [7].

3. Results

3.1. Evaluation of Proportional DENP

The maximum number of drug molecules to be encapsulated in a PDENP is 15000. The maximum flow rate of a drug pump (u_{max}) is set to $1500\ \mathrm{molecule\,s^{-1}}$. This value is relevant since in [4], the rate of the drug pump is $10^6 \mathrm{molecule\,s^{-1}}$ for a nanorobot of $\sim$1 μm in diameter. In this simulation, $k_{L1} = u_{max}/60$, $k_{L2} = 0.1u_{max}/10$, and $k_d = u_{max}$. We consider the effect of PDENPs on the LDL level of the interior of the arterial wall over 24 hours (one day) in two distinguished situations: unhealthy (abnormal) arterial wall where the peak of LDL concentration is $200\ \mathrm{mg\,dL^{-1}}$, and healthy arterial wall where the peak of LDL concentration is $90\ \mathrm{mg\,dL^{-1}}$. Figures 6 and 7 represent the simulation results for these two cases, respectively. The plots of these figures depict the final (controlled) profile of LDL concentration in the arterial wall at the end of 24 hours and compare it with the desired (normal) and uncontrolled (without drug) LDL levels. In the present simulation, the desired LDL level is defined as the equilibrium point of Equation 1 when the concentration of LDL in lumen is $100\ \mathrm{mg\,dL^{-1}}$, corresponding to normal

(optimal) LDL level, and c_{drug} is zero. The uncontrolled LDL level is the initial value of LDL concentration in this simulation and defined as the equilibrium point of Equation 1 when c_{drug} is zero, and the concentration of LDL in lumen is 200 mg dL^{-1} for the unhealthy case (Figure 6), and 90 mg dL^{-1} for the healthy case (Figure 7). Figure 6 demonstrates that although the LDL concentration in lumen is very high (200 mg dL^{-1}), the proposed PDENP could successfully reduce the LDL level in all layers of the arterial wall with reduction rate $(\text{mean}(\frac{\text{uncontrolled level}-\text{controlled level}}{\text{uncontrolled level}}) * 100)$ of 17.9%, 45.7%, 46.9%, and 61.3% in endothelium, intima, IEL, and media, respectively. According to this figure, the controlled LDL level is very close to the desired value in intima, IEL, and media. As it is expected, the controlled LDL level in endothelium is higher than the desired value. This is because of the parameters of the controller such that it does not release any drug in the lumen. Since the range of LDL concentration at the lower positions of endothelium is close to lumen, the PDENP does not release any drug in this place and thus the LDL level is not significantly reduced. Figure 7 demonstrates that the PDENP could successfully understand that the arterial wall is healthy and it should not release drug in this tissue. In this case, the LDL reduction rate is trivial and equals 0.1%, 3.5%, 3.8%, and 8.3% in endothelium, intima, IEL, and media, respectively. The area under the curve of drug-versus-time diagram are 0.00390 μg $mL^{-1}h$ and 0.00035 μg $mL^{-1}h$ in unhealthy and healthy cases, respectively. Comparing these two values shows that the mass of the drug released in unhealthy arterial wall is more than 11 times larger than the healthy wall. This confirms the efficiency of the proposed PDENP in distinguishing between unhealthy and healthy tissues which could significantly reduce the unwanted side effects of drug.

3.2. Evaluation of Sliding-Based Proportional DENP

In this simulation, $u_c = 200$ molecule s^{-1}, $\lambda = 10^{-5}$, and $s_c = 10^{-10}$. We consider the effect of SPDENPs on the LDL level of the interior of an unhealthy arterial wall over 24 hours (one day) where the peak of LDL concentration is 200 mg dL^{-1}. Figure 8 demonstrates that although the LDL concentration in lumen is very high (200 mg dL^{-1}), the proposed SPDENP could successfully reduce the LDL level in all layers of the arterial wall with reduction rate of 14.6%, 50.5%, 51.8%, and 64.4% in endothelium, intima, IEL, and media, respectively.

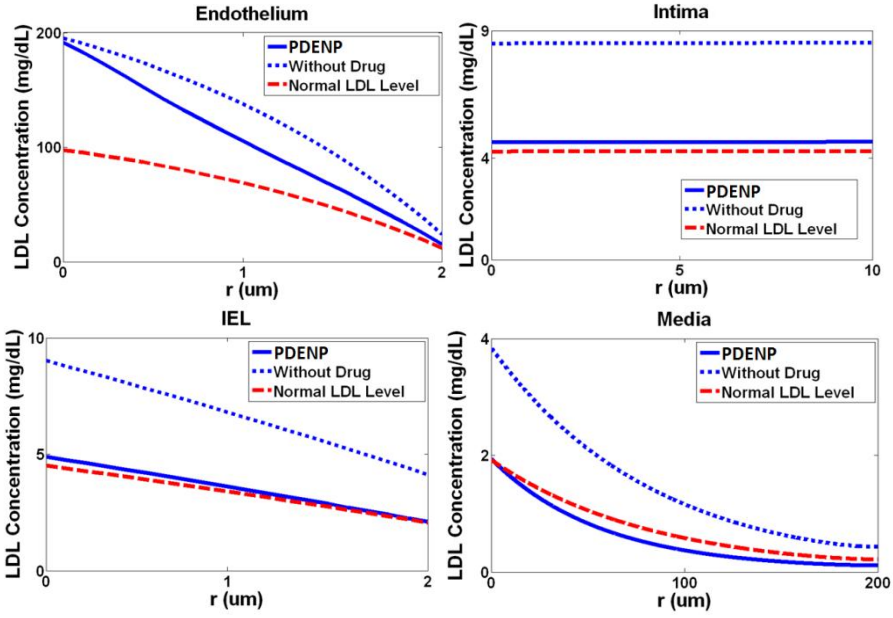

Figure 6. The effect of PDENP on an unhealthy arterial wall (LDL level of 200 mg dL^{-1}) over one day: Final LDL concentration profiles after one day in contrast to normal (desired) and uncontrolled (without drug) LDL levels.

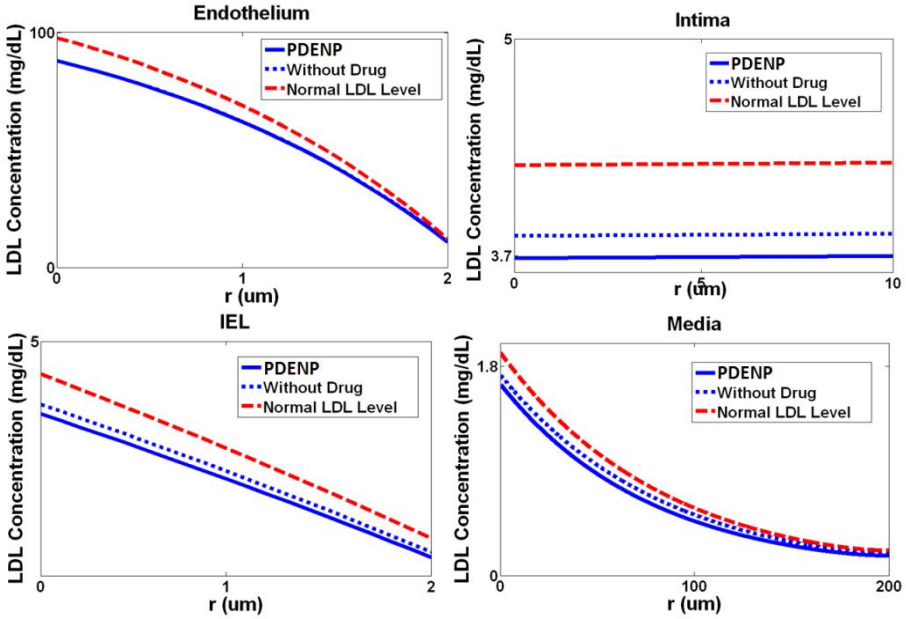

Figure 7. The effect of PDENP on healthy (normal) arterial wall (LDL level of 90 mg dL^{-1}) over one day: Final LDL concentration profiles after one day in contrast to normal (desired) and uncontrolled (without drug) LDL levels.

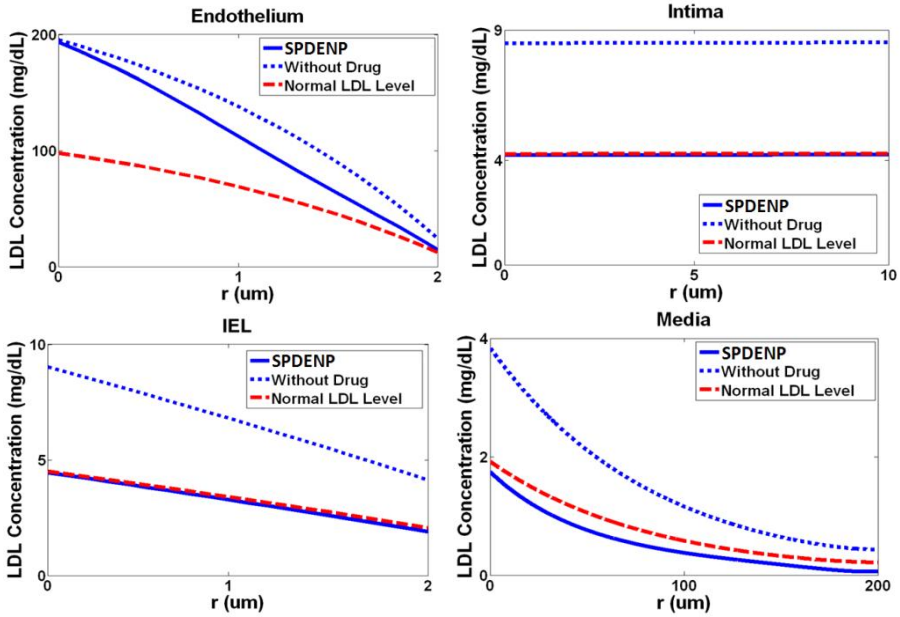

Fig.8. The effect of SPDENP on an unhealthy arterial wall (LDL level of 200 mg dL^{-1}) over one day: Final LDL concentration profiles after one day in contrast to normal (desired) and uncontrolled (without drug) LDL levels.

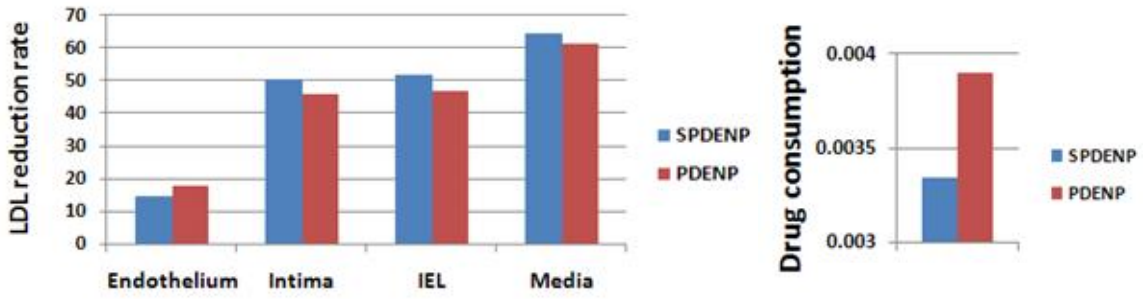

(a) (b)

Fig.9. SPDENP in comparison with PDENP: a) LDL reduction rate in different wall layers, b) Drug consumption.

Comparing these numbers with the results of PDENP shows that SPDENP has better performance in intima, IEL, and media layers (Figure 9). Moreover, the controlled LDL level is even better than the desired value in these three layers. As it is expected, the controlled LDL level in is higher than the desired value. This is because of the parameters of the controller (the condition of $C_{LDL} < 160\,mg\,dL^{-1}$ in Eq.5) such that it does not release any drug in lumen. Since the range of LDL concentration at the lower points of Endothelium is close to the LDL level of lumen, the SPDENP does not release any drug in these points and thus the LDL level is not significantly reduced. The area under the curve of drug-versus-time diagram is $0.00334\ \mu g\,mL^{-1}h$. Comparing this value with the results of PDENP, $0.00390\ \mu g\,mL^{-1}h$, demonstrates that the drug consumption of SPDENP is more efficient than PDENP. Fig.9 illustrates the comparison between SPDENP and PDENP.

4. Discussion

In this paper, a novel non-invasive nanomedical procedure is proposed for prevention of atherosclerosis based on the notion of ADENP. However, the proposed approach is general and can be used for prevention and treatment of different diseases not only limited to atherosclerosis. The hardware complexity of ADENP is much lower than nanorobots, while the performance is maintained by the synergism in the swarm architecture. Since high accumulation of LDL macromolecules within the arterial wall plays a key role in the initiation and development of atherosclerotic plaques, the task of the swarm of ADENPs is autonomous control of LDL level in the interior of the arterial wall. We consider two specific types of ADENPs with distinguishing capabilities, i.e., PDENP and SPDENP. The performance of each type is evaluated and compared with each other on a well-known mathematical model of the arterial wall in the computer simulation environment. Both PDENP and SPDENP could successfully reduce the LDL level in all layers of the arterial wall of a patient with a very high LDL level ($200\,mg\,dL^{-1}$) with reduction rate of 17.9%, 45.7%, 46.9%, and 61.3% for PDENP, and 14.6%, 50.5%, 51.8%, and 64.4% for SPDENP in endothelium, intima, IEL, and media, respectively. Comparing these numbers shows that SPDENP has better performance in reducing the LDL level. Moreover, comparing the areas under the curves of drug-versus-time diagram for these two ADENPs depicts that the drug consumption of SPDENP is more efficient than PDENP. However, in contrast to SPDENP, PDENP is able to automatically distinguish between unhealthy and healthy arterial walls when the mass of the drug released by PDENP in healthy wall is 11 times less than the unhealthy wall.

5. Conclusion

Simulation results demonstrate that the proposed approach can successfully reduce the LDL level to a desired value in the arterial wall of a patient with very high LDL level that is corresponding to the highest rates of cardiovascular disease events. Moreover, it is shown that ADENP is capable of distinguishing between healthy and unhealthy arterial walls to reduce the drug side effects. The different capabilities of PDENP and SPDENP confirm that various types of ADENPs can be designed with special abilities. Generally, the proposed approach can be considered as a promising autonomous non-invasive method to prevent and treat complex diseases such as atherosclerosis.

References

1. Rowhanimanesh A, Akbarzadeh-T M. Control of low-density lipoprotein concentration in the arterial wall by proportional drug-encapsulated nanoparticles. IEEE Trans Nanobioscience. 2012 Dec;11(4):394-401.

2. Hamzah J, Kotamraju VR, Seo JW, Agemy L, Fogal V, Mahakian LM, et al. Specific penetration and accumulation of a homing peptide within atherosclerotic plaques of apolipoprotein E-deficient mice. Proc Natl Acad Sci U S A. 2011 Apr 26;108(17):7154-9.
3. Lu J, Liong M, Li Z, Zink JI, Tamanoi F. Biocompatibility, Biodistribution, and Drug□Delivery Efficiency of Mesoporous Silica Nanoparticles for Cancer Therapy in Animals. Small. 2010;6(16):1794-805.
4. Freitas RA. Pharmacytes: an ideal vehicle for targeted drug delivery. Journal of Nanoscience and Nanotechnology. 2006;6(9-10):9-10.
5. Suraj H, Reddy V, editors. QCA based navigation for nano robot for the treatment of coronary artery disease. Medical Measurements and Applications Proceedings (MeMeA), 2011 IEEE International Workshop on; 2011: IEEE.
6. Hossain S, Hossainy SA, Bazilevs Y, Calo V, Hughes TR. Mathematical modeling of coupled drug and drug-encapsulated nanoparticle transport in patient-specific coronary artery walls. Comput Mech. 2012 2012/02/01;49(2):213-42.
7. S. S. Hossain, S. F. A. Hossainy, Y. Bazilevs, V. M. Calo and T. J. R. Hughes, Mathematical modeling of coupled drug and drug-encapsulated nanoparticle transport in patient-specific coronary artery walls. ICES REPORT 10-41, The Institute for Computational Engineering and Sciences, The University of Texas at Austin, October 2010.
8. S. Martel S, editor. Aggregates of synthetic microscale nanorobots versus swarms of computer-controlled flagellated bacterial robots for target therapies through the human vascular network. Quantum, Nano and Micro Technologies, 2010 ICQNM'10 Fourth International Conference on; 2010: IEEE.
9. Nakano K, Egashira K, Masuda S, Funakoshi K, Zhao G, Kimura S, et al. Formulation of Nanoparticle-Eluting Stents by a Cationic Electrodeposition Coating Technology: Efficient Nano-Drug Delivery via Bioabsorbable Polymeric Nanoparticle-Eluting Stents in Porcine Coronary Arteries. JACC: Cardiovascular Interventions. 2009;2(4):277-83.
10. Nakano M, Matsuura H, Ju D-Y, Kumazawa T, Kimura S, Uozumi Y, et al., editors. Drug delivery system using nano-magnetic fluid. Innovative Computing Information and Control, 2008 ICICIC'08 3rd International Conference on; 2008: IEEE.
11. Dutta A, Mohapatra SS, Sen A, Mukherjee S, editors. Alternative for by-pass surgery using iron-oxide nano-particles. Bio Micro and Nanosystems Conference, 2006 BMN'06; 2006: IEEE.
12. Cavalcanti A, Rosen L, Shirinzadeh B, Rosenfeld M, editors. Nanorobot for treatment of patients with artery occlusion. Proceedings of Virtual Concept; 2006.
13. Cavalcanti A, Freitas Jr RA. Nanorobotics control design: A collective behavior approach for medicine. NanoBioscience, IEEE Transactions on. 2005;4(2):133-40.
14. Cavalcanti A, Shirinzadeh B, Fukuda T, Ikeda S, editors. Hardware architecture for nanorobot application in cerebral aneurysm. Nanotechnology, 2007 IEEE-NANO 2007 7th IEEE Conference on; 2007: IEEE.
15. Cavalcanti A, Shirinzadeh B, Zhang M, Kretly LC. Nanorobot hardware architecture for medical defense. Sensors. 2008;8(5):2932-58.
16. Yang N, Vafai K. Modeling of low-density lipoprotein (LDL) transport in the artery—effects of hypertension. International Journal of Heat and Mass Transfer. 2006;49(5):850-67.
17. American Heart Association. Available at: http://www.heart.org. Accessed Oct 20, 2013.
18. Ai L, Vafai K. A coupling model for macromolecule transport in a stenosed arterial wall. International Journal of Heat and Mass Transfer. 2006;49(9–10):1568-91.
19. Yang N, Vafai K. Low-density lipoprotein (LDL) transport in an artery – A simplified analytical solution. International Journal of Heat and Mass Transfer. 2008;51(3–4):497-505.
20. Li W, Yang Y, Yan H, Liu Y. Three-Input Majority Logic Gate and Multiple Input Logic Circuit Based on DNA Strand Displacement. Nano Letters. [doi: 10.1021/nl4016107]. 2013;13(6):2980-8.
21. Yasuga H, Kawano R, Takinoue M, Tsuji Y, Osaki T, Kamiya K, et al., editors. Logic gate using artificial cell-membrane: NAND operation by transmembrane DNA via a biological nanopore. Micro Electro Mechanical Systems (MEMS), 2013 IEEE 26th International Conference on; 2013 20-24 Jan. 2013.
22. Chan KW, Liu G, Song X, Kim H, Yu T, Arifin DR, et al. MRI-detectable pH nanosensors incorporated into hydrogels for in vivo sensing of transplanted-cell viability. Nature materials. 2013;12(3):268-75.
23. Iscla I, Eaton C, Parker J, Wray R, Kovács Z, Blount P. Improving the Design of a MscL-Based Triggered Nanovalve. Biosensors. 2013;3(1):171-84.
24. Lai J, Shah BP, Garfunkel E, Lee K-B. Versatile Fluorescence Resonance Energy Transfer-Based Mesoporous Silica Nanoparticles for Real-Time Monitoring of Drug Release. ACS nano. 2013;7(3):2741-50.
25. Douglas SM, Bachelet I, Church GM. A logic-gated nanorobot for targeted transport of molecular payloads. Science. 2012;335(6070):831-4.
26. Miyamoto T, DeRose R, Suarez A, Ueno T, Chen M, Sun T-p, et al. Rapid and orthogonal logic gating with a gibberellin-induced dimerization system. Nature chemical biology. 2012;8(5):465-70.

27. Bonnet J, Subsoontorn P, Endy D. Rewritable digital data storage in live cells via engineered control of recombination directionality. Proceedings of the National Academy of Sciences. 2012;109(23):8884-9.
28. Padirac A, Fujii T, Rondelez Y. Bottom-up construction of in vitro switchable memories. Proceedings of the National Academy of Sciences. 2012;109(47):E3212-E20.
29. Jonoska N, Seeman NC. Computing by molecular self-assembly. Interface Focus. 2012;2(4):504-11.
30. Lakin MR, Youssef S, Cardelli L, Phillips A. Abstractions for DNA circuit design. Journal of The Royal Society Interface. 2012;9(68):470-86.
31. Agrawal S, Prajapati R. Nanosensors and their Pharmaceutical Applications: A Review. International Journal of Pharmaceutical Science and Technology. 2012;4:1528-35.
32. Rodríguez-Lorenzo L, de La Rica R, Álvarez-Puebla RA, Liz-Marzán LM, Stevens MM. Plasmonic nanosensors with inverse sensitivity by means of enzyme-guided crystal growth. Nature materials. 2012;11(7):604-7.
33. Khanna VK. Nanosensors: Physical, Chemical, and Biological: Taylor & Francis; 2011.
34. Du L, Song H, Liao S. A biocompatible drug delivery nanovalve system on the surface of mesoporous nanoparticles. Microporous and Mesoporous Materials. 2012;147(1):200-4.
35. Yu-Long S, Ying-Wei Y, Wei W, Xiao-An ZS. Supramolecular nanovalve systems based on macrocyclic synthetic receptors. Chemical Journal of Chinese Universities. 2012;33(8): 1635-42.
36. Xue M, Findenegg GH. Lysozyme as a pH-Responsive Valve for the Controlled Release of Guest Molecules from Mesoporous Silica. Langmuir. 2012;28(50):17578-84.
37. Tamsir A, Tabor JJ, Voigt CA. Robust multicellular computing using genetically encoded NOR gates and chemical 'wires'. Nature. 2011 Jan 13;469(7329):212-5.
38. Qian L, Winfree E. Scaling up digital circuit computation with DNA strand displacement cascades. Science. 2011;332(6034):1196-201.
39. Qian L, Winfree E. A simple DNA gate motif for synthesizing large-scale circuits. DNA computing: Springer; 2009. p. 70-89.
40. Al-Fandi M, Jaradat MA, Al-Rousan M, Jaradat S, editors. A living biological nano robot as self-navigator sensor for diseases. Biomedical Engineering (MECBME), 2011 1st Middle East Conference on; 2011: IEEE.
41. Yang LM, Blount P. Manipulating the permeation of charged compounds through the MscL nanovalve. FASEB J. 2011 Jan;25(1):428-34.
42. Freitas Jr RA, Havukkala I. Current status of nanomedicine and medical nanorobotics. J Comput Theor Nanosci. 2005;2(1):1-25.
43. Sinden RR. DNA Structure and Function: Academic Press; 1994.
44. Yamada H, Urata C, Ujiie H, Yamauchi Y, Kuroda K. Preparation of aqueous colloidal mesostructured and mesoporous silica nanoparticles with controlled particle size in a very wide range from 20 nm to 700 nm. Nanoscale. 2013 Jul 7;5(13):6145-53.
45. Rowhanimanesh A. Swarm control systems for nanomedicine and its application to the prevention of atherosclerosis. PhD Dissertation of Control Engineering, Faculty Advisor: Prof. M-R. Akbarzadeh-T., Ferdowsi University of Mashhad; 2013.
46. Gazi V, Passino KM. Swarm stability and optimization: Springer; 2011.
47. Gazi V, Fidan B, Hanay YS, Köksal MI. Aggregation, foraging, and formation control of swarms with non-holonomic agents using potential functions and sliding mode techniques. Turk J Elec Engin. 2007;15(2):149-68.
48. Gazi V. Swarm aggregations using artificial potentials and sliding-mode control. Robotics, IEEE Transactions on. 2005;21(6):1208-14.
49. Gazi V, Passino KM. Stability analysis of swarms. Automatic Control, IEEE Transactions on. 2003;48(4):692-7.
50. Seibold B. A compact and fast MATLAB code solving the incompressible Navier-Stokes equations on rectangular domains, http://www-math.mit.edu, March. 2008;31:2008.